Journal of large-scale research facilities

Journal of large-scale research facilities, 2, A90 (2016) http://dx.doi.org/10.17815/jlsrf-2-86

Published: 16.11.2016

SPEEM: The photoemission microscope at the dedicated microfocus PGM beamline UE49-PGMa at BESSY II

Helmholtz-Zentrum Berlin für Materialien und Energie *

Instrument Scientists:
- Dr. Florian Kronast, , Helmholtz-Zentrum Berlin für Materialien und Energie
  phone: +49 8062-14620, email: florian.kronast@helmholtz-berlin.de
- Dr. Sergio Valencia Molina, Helmholtz-Zentrum Berlin für Materialien und Energie
  phone: +49 8062-15619, email: sergio.valencia@helmholtz-berlin.de

Abstract: The UE49-PGMa beamline hosts a photoemission electron microscope (PEEM) dedicated to spectromicroscopy and element-selective magnetic imaging on the nanometer scale. The instrument is an Elmitec PEEM III equipped with energy filter and Helium cooled manipulator. Laser driven excitations can be studied using an attached Ti:Sa laser. A variety of customized sample holders is available for imaging in moderate magnetic / electric field, temperature control, or local laser excitations. With x-rays the instrument is capable of 30 nm spatial resolution.

1 Introduction

Magnetic nanostructures are at the heart of modern data storage technology. Typical dimensions of magnetic bits are in the sub-100 nm region. In addition novel magnetoelectronics devices such as magnetic random access memory junctions are operated on the sub-100 nm m scale. An understanding magnetic properties of such low-dimensional structures is only accessible to spectro-microscopy tools capable of appropriate lateral resolution. This goal is achieved by combining a photoemission microscope (SPEEM) with a dedicated microfocus PGM beamline (UE49 PGM). High photon flux in combination with full polarization control makes this setup the ideal tool for space resolved and element selective investigation of nanostructures by means of chemical maps (X-ray absorption spectroscopy (XAS)) and magnetic imaging (X-ray magnetic circular dichroism (XMCO) and X-ray magnetic linear dichroism (XMLD)).

*Cite article as: Helmholtz-Zentrum Berlin für Materialien und Energie. (2016). SPEEM: The photoemission microscope at the dedicated microfocus PGM beamline UE49-PGMa at BESSY II. *Journal of large-scale research facilities, 2*, A90. http://dx.doi.org/10.17815/jlsrf-2-86

Figure 1: Photograph of the SPEEM setup.

2 Instrument application

The particular strength of this instrument is the element specificity and quantitative magnetic contrast at high spatial resolution in combination with a variable sample environment. The instrument has been equipped with a LHe cryostat for sample temperatures down to 45 K. Special sample holders have been developed. Some of them combine temperature control in a range from 45 K to 600 K with the application of magnetic fields of up to 75 mT and a voltage applied to the sample during imaging (Sandig et al., 2012). Customized power supplies and a dedicated software control allows for special features, such as lens tracking during application of magnetic or electric field, on-the-fly data recording, sub Kelvin temperature control and stabilization, or macro based data acquisition. A Ti:Sa laser system attached to the microscope can be used to study laser driven effects such as phase changes or magnetic switching. Diffraction limited laser spot sizes can be reached with a dedicated sample holder (Gierster, Pape, et al., 2015).

Different modes of operation are possible. Imaging of secondary electrons allows for XAS spectroscopy or magnetic imaging with XMCD or XMLD contrast. Due to an energy filter also spatially resolved photo electron spectroscopy (XPS) and even angle resolved photo emission spectroscopy (micro ARPES) at kinetic energies of up to 1000 eV is possible. Even depth resolved XPS using the standing wave technique can be done (Gray et al., 2010; Kronast et al., 2008). At typical working conditions of the microscope the field of view is about 3 −10 µm and matches ideally with the x-ray spot size of 10x20 µm. The photon flux provided by the 1200 l/mm grating allows electron count rates close to the space charging limit and is sufficient to optimize spatial resolution and collection efficiency. Frame rates of 1-3 s at 5 µm field of view are possible. Some examples of typical applications are listed below:

- Chemical maps by XAS and XPS (Fang et al., 2014; Moreno et al., 2010)
- Magnetic domain imaging by XMCD and XMLD (Boeglin et al., 2009)
- Phasetransitions / temperature dependent measurements (Ewerlin et al., 2013)
- Field dependent measurements (Kronast et al., 2011)
- Micro-spectroscopy on nanostructures, magnetic responses and interactions, probing of core shell structures (Kimling et al., 2011)
- Magnetic transport and spin torque (Heyne et al., 2010)
- Magnetic/magnetoelectric coupling in thin films and multifoerroics (Cherifi et al., 2010)

- Laser induced magnetic switching or phase changes (Gierster, Ünal, et al., 2015)
- Time-resolved magnetization dynamics (fs-laser pump, X-ray probe) (Miguel et al., 2009)

3 Source

The insertion device is the elliptical undulator UE49 with the following parameters:

Type	APPLE2
Location	L108
Periode length	49 mm
Periods/Pols	64 n
Minimal Energy at 1,7 GeV	91.2 eV
Minimal Gap	16 mm
Polarisation	linear variable 0° ... +90° elliptical, circular

Table 1: Parameters of insertion device UE49.

4 Optical design

The UE49-PGMa beamline is one of three branches at the UE49 insertion device, an Apple II-type undulator with full polarization control. For highest brilliance the UE49 is located in one of the low-beta sections of the BESSY II storage ring. A schematic layout of the UE49-PGMa beamline is shown in Figure 2. The beamline comprises five optical elements, four mirrors and one grating. The cylindrical mirror M1 and the toriodal mirror M3 serve as switching mirror units and distribute the beam to neighboring branches. M4 is an ellipsoidal refocussing mirror, optimized for high transmittance and small spot size. The x-ray spot on the sample is a de-magnified image of the exit slit. At an incidence angle of 74° and a slit opening of 200 µm the spot measures 20 µm in horizontal and 10 µm in vertical direction (FWHM). The beamline is equipped with a plane grating monochromator that covers an energy range from 80 to 1800 eV. With the finest grating (1200 l/mm) a spectral resolution $(E/\Delta E)$ of 10000 at 700 eV can be achieved. The photon flux ranges from 10^{11} to 10^{13} ph/s/100 mA. A detailed flux table for this grating is shown in Figure 3. Using different gratings with a lower line density (600 l/mm and 300 l/mm) the photon flux can be increased at the expense of spectral resolution. Main parameters of the UE49-PGMa beamline are summarized in Table 1 and Table 2.

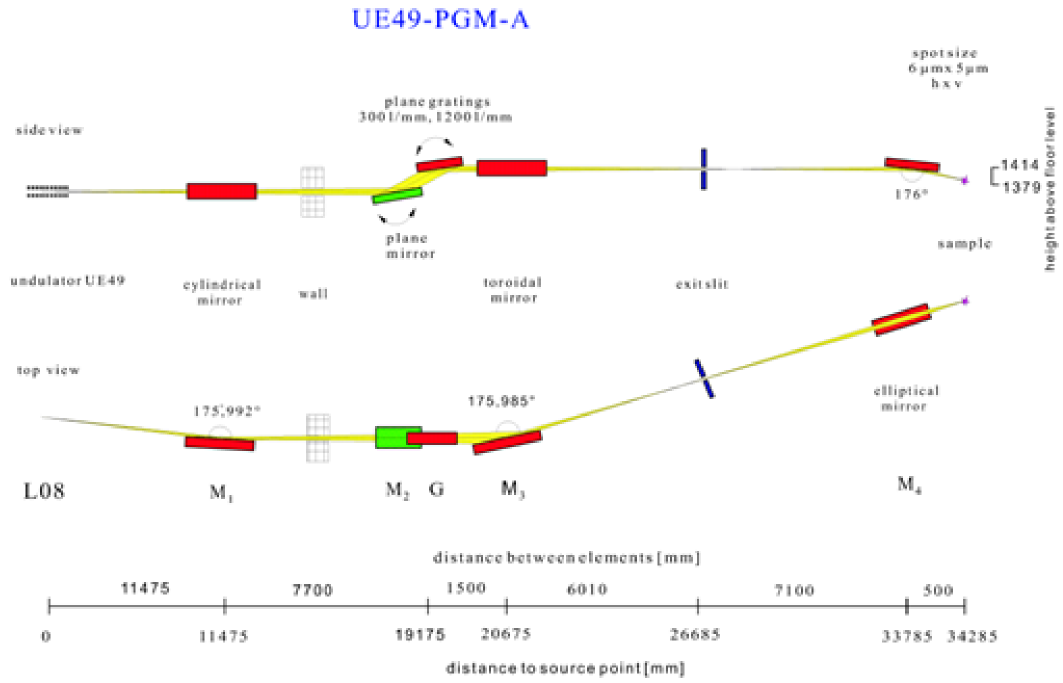

Figure 2: Optical layout of beamline UE49-PGMa.

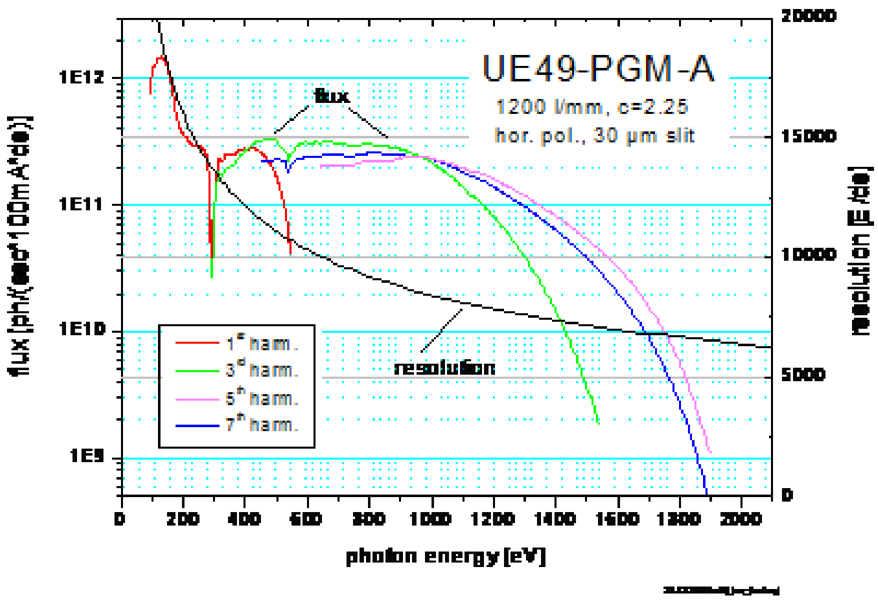

Figure 3: Photon flux measured with the 1200l/mm grating.

5 Technical Data

SPEEM Microscope	
Spatial resolution	25 nm
Energy analyzer	E < 0.3 eV
Monochromator	PGM
Azimuthrotation	Yes
Temperatur control	45 - 600 K
Electric and magnetic field	max. 75 nT during imaging
Beamline	
Monochromator	PGM
Energy range	80 to 1800 eV
Energy resolution	10.000 at 700 eV
Spot size on sample	10 x 20 µm
Full polarization control	Yes
Fixed endstation	Yes
Preparationchamber	Evaporation Fe, Co, Ni, Al... Ion sputtering Sample storage in vacuum up to 6
Pump Laser	800 nm wavelength 300 nJ max. pulse energy 80 fs pulse duration Repetition rate variable from single pulse to 2.5 MHz

Table 2: Technical parameters for the SPEEM station and the UE49-PGMa beamline

References

Boeglin, C., Ersen, O., Pilard, M., Speisser, V., & Kronast, F. (2009). Temperature dependence of magnetic coupling in ultrathin NiO/$Fe_3O_4(001)$ films. *Phys. Rev. B*, *80*, 035409. http://dx.doi.org/10.1103/PhysRevB.80.035409

Cherifi, R. O., Ivanovskaya, V., Phillips, L. C., Zobelli, A., Infante, I. C., Jacquet, E., … Bibes, M. (2010). Electric-field control of magnetic order above room temperature. *Phys. Rev. Lett.*, *105*, 187203. http://dx.doi.org/10.1103/PhysRevLett.105.187203

Ewerlin, M., Demirbas, D., Brüssing, F., Petracic, O., Ünal, A. A., Valencia, S., … Zabel, H. (2013). Magnetic dipole and higher pole interaction on a square lattice. *Phys. Rev. Lett.*, *110*, 177209. http://dx.doi.org/10.1103/PhysRevLett.110.177209

Fang, H., Battaglia, C., Carraro, C., Nemsak, S., Ozdol, B., Kang, J. S., … Javey, A. (2014). Strong interlayer coupling in van der Waals heterostructures built from single-layer chalcogenides. *Proceedings of the National Academy of Sciences*, *111*(17), 6198-6202. http://dx.doi.org/10.1073/pnas.1405435111

Gierster, L., Pape, L., Ünal, A. A., & Kronast, F. (2015). A sample holder with integrated laser optics for an ELMITEC photoemission electron microscope. *Review of Scientific Instruments*, *86*(2). http://dx.doi.org/10.1063/1.4907402

Gierster, L., Ünal, A., Pape, L., Radu, F., & Kronast, F. (2015). Laser induced magnetization switching in a TbFeCo ferrimagnetic thin film: discerning the impact of dipolar fields, laser heating and laser helicity by XPEEM. *Ultramicroscopy*, *159, Part 3*, 508 - 512. http://dx.doi.org/10.1016/j.ultramic.2015.05.016

Gray, A. X., Kronast, F., Papp, C., Yang, S.-H., Cramm, S., Krug, I. P., … Fadley, C. S. (2010). Standing-wave excited soft x-ray photoemission microscopy: Application to co microdot magnetic arrays. *Applied Physics Letters*, *97*(6). http://dx.doi.org/10.1063/1.3478215

Heyne, L., Rhensius, J., Ilgaz, D., Bisig, A., Rüdiger, U., Kläui, M., … Kronast, F. (2010). Direct determination of large spin-torque nonadiabaticity in vortex core dynamics. *Phys. Rev. Lett.*, *105*, 187203. http://dx.doi.org/10.1103/PhysRevLett.105.187203

Kimling, J., Kronast, F., Martens, S., Böhnert, T., Martens, M., Herrero-Albillos, J., … Meier, G. (2011). Photoemission electron microscopy of three-dimensional magnetization configurations in core-shell nanostructures. *Phys. Rev. B*, *84*, 174406. http://dx.doi.org/10.1103/PhysRevB.84.174406

Kronast, F., Friedenberger, N., Ollefs, K., Gliga, S., Tati-Bismaths, L., Thies, R., … Farle, M. (2011). Element-specific magnetic hysteresis of individual 18 nm Fe nanocubes. *Nano Letters*, *11*(4), 1710-1715. http://dx.doi.org/10.1021/nl200242c

Kronast, F., Ovsyannikov, R., Kaiser, A., Wiemann, C., Yang, S.-H., Bürgler, D. E., … Fadley, C. S. (2008). Depth-resolved soft x-ray photoelectron emission microscopy in nanostructures via standing-wave excited photoemission. *Applied Physics Letters*, *93*(24). http://dx.doi.org/10.1063/1.3046782

Miguel, J., Sánchez-Barriga, J., Bayer, D., Kurde, J., Heitkamp, B., Piantek, M., … Kuch, W. (2009). Time-resolved magnetization dynamics of cross-tie domain walls in permalloy microstructures. *Journal of Physics: Condensed Matter*, *21*(49), 496001.

Moreno, C., Munuera, C., Valencia, S., Kronast, F., Obradors, X., & Ocal, C. (2010). Reversible resistive switching and multilevel recording in La0.7Sr0.3MnO3 thin films for low cost nonvolatile memories. *Nano Letters*, *10*(10), 3828-3835. http://dx.doi.org/10.1021/nl1008162

Sandig, O., Herrero-Albillos, J., Römer, F., Friedenberger, N., Kurde, J., Noll, T., … Kronast, F. (2012). Imaging magnetic responses of nanomagnets by XPEEM. *Journal of Electron Spectroscopy and Related Phenomena*, *185*(10), 365 - 370. http://dx.doi.org/10.1016/j.elspec.2012.07.005